Egyptian Geophysical Society
EGS Journal, vol. 7, No. 1, 71-82 (2009)

USE OF AEROMAGNETIC DATA IN THE INTERPRETATION OF THE STRUCTURAL FRAMWORK OF EAST ASWAN AREA, SOUTHERN EASTERN DESERT, EGYPT.

M.M. ELTARRAS

Nuclear Materials Authority, P. O. Box 530 El- Maadi, Cairo, Egypt

استخدام بيانات المغناطيسية الجوية لتفسير الشكل التركيبى لمنطقة شرق أسوان، جنوب الصحراء الشرقية، مصر

الخلاصة: تم تحديد الإطار التركيبي لمنطقةِ شرق أسوان والتي تقع بين خطى عرض ٤٥′ ٢٣° و٧ ′ ٢٤° شمالا و خطى طول ٥٥′ ٣٢° و ٤٥′ ٣٣° شرقا جنوب الصحراء الشرقية ، مصر، تغطى منطقة البحث حوالي ١٩٠٠كم٢ تقريبا. ولقد تم هذا من خلال تطبيق وتكامل بعض التقنيات التفسيرية المتقدّمةِ لبياناتِ الخريطة الجوية المغناطيسية الكلية المحولة إلى القطب الشمالي للأرض. تتضمّنُ هذه التقنياتِ تقنية طيف القدرة، و قد تم فصل المجال المغناطيسي للتمييز بين مصادر الشاذات و التباينات الضحلة (المتبقية أو القريبة من السطح) والعميقة (الإقليمية أو الغائرة فى العمق)، و تقنية ألاستمرارية لأعلى، و تقنية المشتقة الرأسية الثانية، و تقنية تحليل الإشارة.
وقد أدى التكامل بين تطبيق هذه التقنيات الخمس إلى رسم خريطة تركيبة لصخور القاعدة المعقدة كمنتج نهائي لتوضيح الإطار الجيولوجي والتركيبي الإقليمي العام لمنطقة البحث ووجد أن عناصر التراكيب التي أثرت في منطقة الدراسة عبارة عن صدوع وطيات. هذا وقد تم تطبيق طريقة التحليل الاتجاهى وذلك باستخدام تقنية الأشكال النجمية على نتائج الخريطة التركيبة لصخور القاعدة المعقدة، كان من نتائج تطبيق هذه الطريقة ظهور أربع وجهات مغناطيسية (تركيبية) رئيسية ذات مغزى ومؤثرة على بنية منطقة البحث وهى وجهات: شمال الغرب، وشمال الشرق، وغرب شمال الغرب وشمال شمال الشرق ولقد وجد أن هذه الوجهات المغناطيسية (البنيوية) تتماثل إلى حد بعيد مع الواجهات التي توصل إليها العديد من العلماء المهتمين بجيولوجية الصحراء الشرقية لمصر.

ABSTRACT: *The delineation of gross structural framework of East Aswan area, located between latitudes 23°45′ - 24°07′N and longitudes 32°55′ - 33°24′E southern Eastern Desert of Egypt, was reached through the integration of some interpretation techniques applied to the aeromagnetic survey data reduced to the pole (RTP). These techniques are power spectrum technique, regional-residual separation, upward continuation, second vertical derivative and analytical signal. The results obtained from the various interpretation techniques were used in an integrated manner to construct the interpreted magnetic basement structural map. The structural elements affecting the study area include faults and folds (down faulted and uplifted block). Trend analysis techniques were applied on the resultant structural elements, to define the significant and predominant tectonic trends affecting on the study area, that are responsible for the structural development of its geological units. As a result of the application of the rose diagram for the main trends proved to be significant. Those trends are sorted from the strongest to the weakest as NW, NE, WNW and NNE.*

1. INTRODUCTION

East Aswan area is located in the southern Eastern Desert covering a total surface area of about 1900 km^2. It is bounded by latitudes 23° 45′ - 24° 07′ N and longitudes 32° 55′ - 33° 24′ E (Fig. 1). The study area is formed from rocks belonging to the Nubian sandstone (NSS) series (mainly sandstone and shales) and igneous rocks mainly granites and metasediment rocks. Besides, in some places, these rocks are traversed by dykes of diorite penetrating the basement rocks and NSS in thin bands, exposed in deeper valleys.

Topographically, the area is relatively a flat desert plateau with irregular hills. It is an extensively dissected plateau varying in altitude from about 150 meters above sea level (asl) near Aswan (northwestern side of the area understudy) to about 430 meters (asl) at the eastern side.

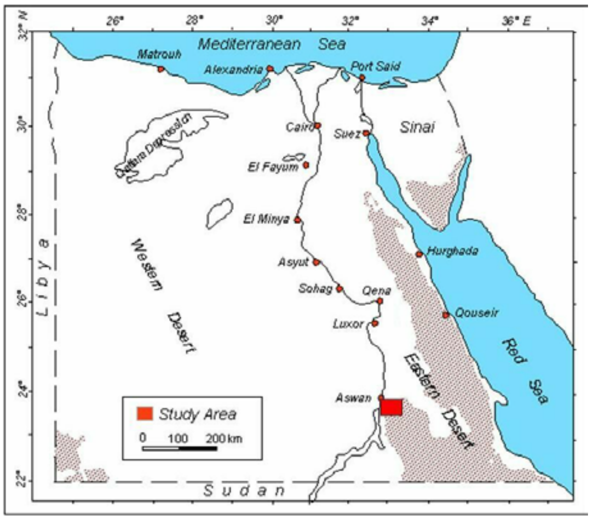

Fig. (1): Location map of the study area.

The rocks of the study area are dissected by several wadies (dry valleys) and their tributaries, the majority of which strike in NW, NNE, and NE directions. These wadis are generally structurally controlled by fracture system trending in NW, NNE, and NE, directions.

The airborne survey of the study area has been provided through the MPGAP program (Aero Service report, Western Geophysical Company of America in 1984). The study area is part of what is referred to as the survey area II. The survey was flown with a geo-physically equipped Cessna 404 Titan aircraft at a barometric altitude of 120 meters above ground level. The data was acquired along parallel flight lines oriented in a NE-SW direction at one kilometer spacing, while the tie lines are spaced at 10 km directed in NW-SE direction. The collected spectral gamma-ray measurements were corrected, compiled and finally displayed in the form of composite stacked profiles and contour maps showing the total magnetic field intensity measurements (Tf in nT).

2. Geological Outline

The investigated area represents a sample area from the south eastern desert of Egypt is covered by both basement complex of Precambrian age and phanerozoic cover sediments of upper Cretaceous and Quaternary age (Fig. 2). The Precambrian basement is uncomfortably overlaid by the Nubian formation whose sediments range in age from Late Cretaceous to Eocene. Quaternary deposits (Issawi, 1978 &1982). The basement complex of Egypt attains the attention of many authors such as El Shazly (1964 &1977), El Gaby et al. (1988 & 1990). The rock units in the study area can be chronologically grouped into the following main rock sequence according to the classification of Takla and Hussein classification (1995), the different rock units exposed in East Aswan area are chronologically grouped into three main groups consistent with the following sequence starting from the oldest: -

2.1- Ophiolitic mélange and island arc association

These rocks represent the oldest rocks in the study area. It represented by one rock units metasediments, which have been subjected to low to moderate – grade metamorphism and to folding. They cover most of the northwestern and northeastern parts of the mapped area. They include some schists, mudstones, and greywacks of volcanogenic composition. The whole sequence of metasediments is folded and sheared. They also exhibit extensive foliation while in some outcrop some of the primary structures are still presented displaying intense fold structures (El Ramly and Akaad, 1960). These rocks cover the most the northwestern, and northeastern parts of the mapped area.

2.2- Continental margin-within plate magmatism and sedimentation

These rocks are mainly represented by intrusive granites possing relatively sharp contacts with the surrounding rocks and are followed by the formation of pegmatites, aplites, felsites and quartz veins (Ghanem, 1978). They have been emplaced over a wide range of time, however, their majority are believed to be formed by the end of Late Precambrian time (El-Shazly, 1964 and 1977). These rocks are exposed mainly in the central and western parts of the study area and invade the metasediments country rocks (Fig. 2). Pink granites form large batholiths in the eastern desert. These granites are calcalkalic in composition, in which the potash feldspars are predominant while orthoclase is uncommon, with equigranular texture (El Shazly, 1977).

2.3- The Phanerozoic Sediments

The foreland sediments of the area are represented by the Cretaceous Nubian Sandstone (NSS) formation and the Quaternary deposits. The NSS is located at the extreme of northeastern and west center of the mapped area and uncomfortably overlain the basement rocks (Fig.2). Attia (1955) concluded that the NSS of the east of Aswan is of marine origin and the deposition of the strata began under shallow water conditions, the continent was not far away and the area must have been subjected to the uplift and subsidence. The NSS was deposited during a long interval of the geological time from the Paleozoic, Pre-Carboniferous until the Upper Cretaceous (Farag, 1958).

The Quaternary – wadi deposits are the youngest sediments recorded in the study area. It consists of detritus, sand pebbles and rare boulders distributed over the study area and constitute the surficial cover in the main wadis and tributaries. These deposits are referred to as Pleistocene and Recent deposits (coastal plain deposits). They are generally formed by the weathering of the local and adjacent rocks and their accumulation during the Quaternary time.

3. Aim of Study

The present study is an attempt to make use of the available aeromagnetic survey data, as a main source of information, aided by the geological knowledge to figure out the gross structural framework of the study area and to define the significant tectonic trends that are responsible for the structural development of its geological units. The application of various methods and interpretation techniques of analysis to the aeromagnetic data in such an area characterized by widely varying geological rock units and structures, would permit the elucidation of near-surface and deep-seated geological and structural configuration of the study area. In order to pursue these objectives, the total aeromagnetic map reduced to the north magnetic pole (RTP) has been subjected to various methods of analysis including the following techniques of interpretation.

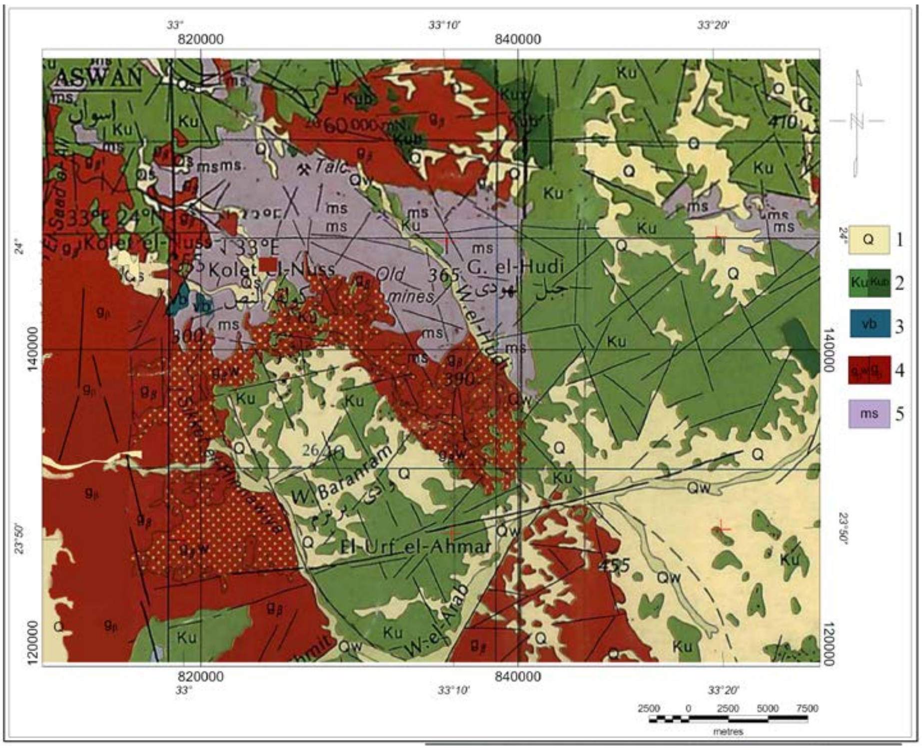

Fig. (2): Geologic map of the study area (after Conoco Inc. 1989).

1) Quaternary Deposits 2) Nubian Sandstone
3) Tertiary Volcanics 4) Younger Granites
5) Metasediments

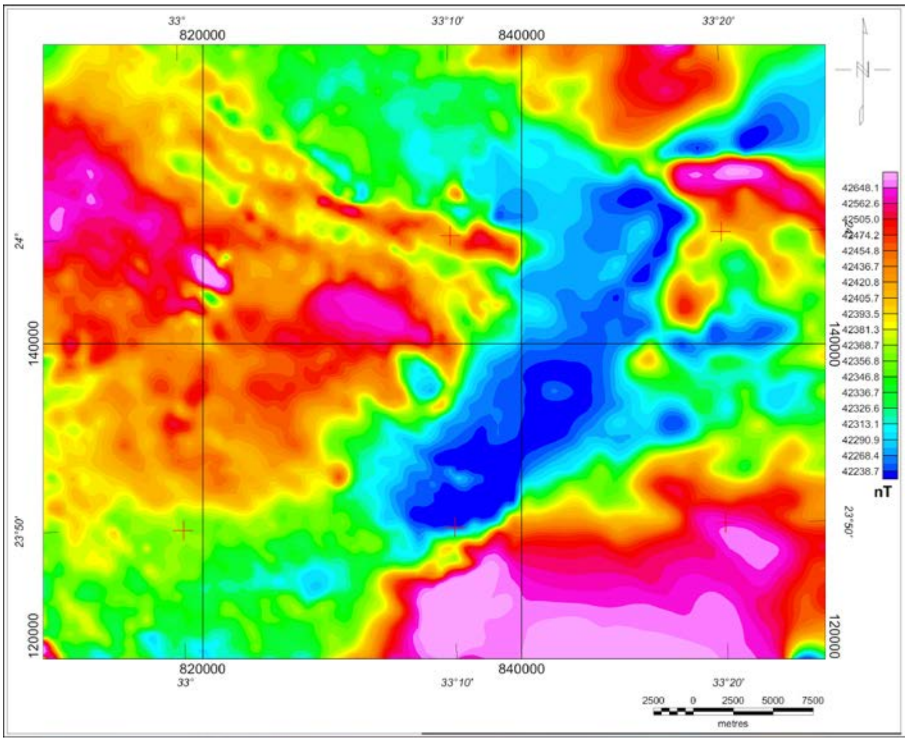

Fig. (3): RTP total magnetic intensity map (Aero-Service, 1984).

4. Analysis techniques of aeromagnetic data

To separate the regional and residual components of the magnetic data, the two dimensional power spectrum was calculated from the R.T.P. magnetic map (Fig. 3). The power spectrum (Fig. 4) shows two linear segments related to regional and residual components at average depth of 1.0 and 2.0 km respectively. Moreover, the analysis of the power spectrum curve (Fig. 3) shows that the deep-seated magnetic component frequency varies from 0.05 to 0.1 cycle/km. Meanwhile the near-surface magnetic component frequency ranges from 0.1 to 0.26 cycle/km. These bands of frequency were used through the band pass filter technique to produce the regional and residual magnetic component maps.

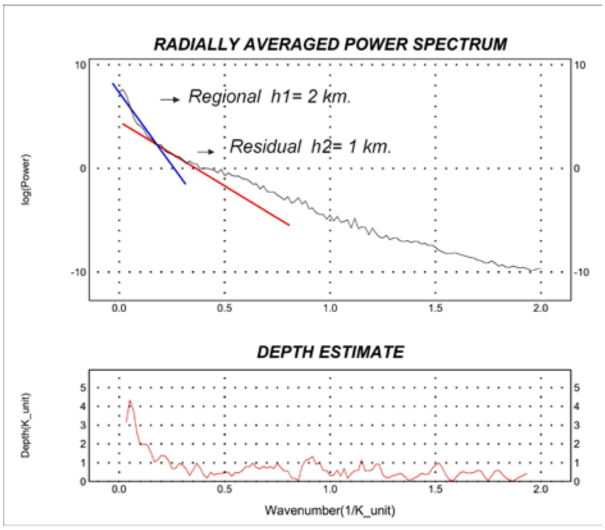

Fig. (4): Power spectrum of the RTP magnetic map (Fig. 3).

Several advanced techniques have been developed for the analysis of aeromagnetic maps, which led finally to their quantitative interpretation. The following are some of these quantitative techniques, which are applied to delineate the geologic structure of the area under investigation with a better accuracy.

4.1- Calculation of Power Spectrum for interface determination

An efficient method of computing spectrum and cross - spectrum of large-scale aeromagnetic field data has been developed and programmed for a digital computer by Naidu (1969). Cianciara and Marcak (1976) made an interpretation of the gravity anomalies by means of local power spectrum. Cianciara and Marcak (1979) also used the power spectrum technique for filtering aeromagnetic data. In the present study, the interface determination, isolation of the magnetic anomalies into regional and residual components and calculation of magnetic gradient were carried out using the local power spectrum technique of Cianciara and Marcak (1979). The magnetic data shows the broad effects of the deep- seated (regional) features, as well as the stronger and more localized effects of the shallower near- surface (residual). Meanwhile, the residual anomalies are superimposed on the regional magnetic pattern and are characterized by small closure, noses with accompanying flattening and steeping of the contours (Dobrin, 1976).

4.2- Normalized horizontal gradient of the field intensity

Horizontal gradient is a simple approach to locate linear structures such as contacts and faults from potential field data. For magnetic field *M(x,y)*, the horizontal gradient magnitude *HG(x,y)* is given by (Cordell and Grauch, 1982, 1985)

$$HG(x,y)=\sqrt{\left(\frac{\partial M}{\partial x}\right)^2+\left(\frac{\partial M}{\partial y}\right)^2} \qquad (1)$$

This function is peaked over magnetic contacts under certain assumptions: (1) the magnetic field and source magnetization are vertical, (2) the contact is vertical and (3) the sources are thick (Phillips, 1998). Violation of the first two assumption leads to shift of the peaks away from the contact location. Violation of the third assumption leads to secondary peaks parallel to the contacts. In order to partially satisfy the first two assumptions, the method were applied to the regional component of the reduced to the pole magnetic data. To represent the distribution of isolines of the magnitude of the horizontal gradient in the area under study, the horizontal magnetic field intensity was calculated and represented in the form of contour map. The method is especially useful in the case of faults or discontinuities and folds, where the isolines of horizontal magnetic gradient are closed near the plane of the fault discontinuity.

4.3- Upward continuation techniques

The upward continuation is the process by which the magnetic field data are analytically projected from one datum surface upward to other surfaces above the original datum, i.e. mathematically transformed into what it would be if it would have been measured above the earth's surface. It can be applied to magnetic field data to obtain reasonably accurate representation of the total. field intensity at a higher level (Telford, 1987). In the present study, the continuation coefficients are calculated using upward continuation in frequency domain. The frequency domain gives much simpler expression for the fields and allows immediate recognition of the convolution factors (Gunn, 1975).

4.4- Vertical derivative

The SVD is used in the present work to locate edges of magnetic bodies and to emphasize sources at shallow depth. The features of interest in the SVD map are the maximum and the zero contours. The closed zero contours outlines the magnetic bodies, and the distance from the SVD maxima to the zero contour is a measure of the depth to the top of the causative body using the method of Vaquier et al., (1963). The measured distances between curvature maxima and zero contour lines could be converted to depths to the buried magnetic bodies. Henderson and Zietz (1949) proved also that the spacing of the grid lines did not significantly affect the location of zero, maximum and minimum values of the curvature for the theoretical bodies, however, smaller grid spacing result in a more accurate delineation of the curvature.

The importance of this technique for magnetic interpretation arises from the fact that the double differentiation with respect to depth tends to emphasize the smaller, shallower geologic anomalies at the expense of larger, regional features. The second vertical derivative picture of the anomalies which are important in oil and mineral exploration than is the original magnetic picture, (Elkins, 1951). Finally, in the area under study the individual anomalies were isolated and identified with theoretical models. The appropriate distances were measured, and then the depths obtained from the intensity curves were verified and supplemented.

4.5- Analytical Signal

The analytical signal is virtually independent of the inclination of magnetization and is thus a better toll than reduction to the pole for interpretation of magnetic anomalies in middle and low latitude (Shuang Qin, 1994). The analytical signal further turns both negative and positive anomalies into a positive response which is directly above the magnetic source. It is independent of the remnant magnetization and direction of the inducing field. The 3-D magnetic analytical signal amplitude is related to the magnetic contrast of the underlying rocks. The map of the analytical signal can be used to outline the edges of magnetic sources. The analytic signal is normally derived from the three orthogonal gradients of the total magnetic field using the expression (MacLeod et al., 1993):

$$|A\ (x, y)| = [(dT/dX)^2 + (dT/dY)^2\ (dT/dZ)^2]^{½} \qquad (2)$$

where A(x, y) is the amplitude (or the absolute value) of the analytical signal at (x, y) and T is the observed magnetic field at (x, y). The amplitude of the 3-d analytical signal of the total magnetic field is positive regardless of the direction of magnetization; the amplitude being proportional to the magnetization contrast of the underlying rocks. Thus the 3-D analytic signal shows the edges of magnetic bodies, which these edges represent rock contacts, can be roughly interpreted as “pseudo-geology” map if the magnetic units outcrop.

5. RESULTS AND DISCURSION

The first impression from looking at the RTP aeromagnetic map (Fig. 3) of the study area is that it dose not agree well with the surface lithologies on the geological map (Fig. 2). Close inspection of the RTP magnetic map (Fig. 3) and the regional (deep-seated) filtered magnetic map (Fig. 5) shows that the area under consideration could be zoned-magnetically-into four different zones having various magnetic characters. Three of the identified magnetic zones are represented mainly by positive anomalies while the fourth zone is represented by negative anomaly zone. The first wide anomaly zone extends from the centeral to the extreme weast of the map, it is represented by a broad and huge of positive magnetic anomalies extending in nearly NW to WNW direction. This zone is connected on surface geology with younger granite and metasediments. The second positive zone at the southeastern part of the mapped area is represented by incomplete positive magnetic anomaly (huge zone). It is associated on surface geology with younger granite and shallower NSS. This zone extends nearly in EW direction. The third positive anomaly zone is represented by two circular anomalies at the northeastern part of the mapped area reaching more than 2647nT. These positive magnetic anomalies varying much in their amplitudes, wavelengths and sizes. The variation in amplitude of these anomalies may reflect changes in the composition of the intrusive bodies. Meanwhile, the difference in sizes of these anomalies reflects the sizes of these intrusions. Furthermore, the variations in the wavelengths indicate the variations in the depths of their causative intrusions or bodies.

The negative magnetic zone occupies the majority of the central part of the investigated area and is represented by a broad and huge belt of negative magnetic anomalies that extend from the centeral to the extreme south and northwestern parts of the mapped area with maximum amplitude at the centeral of the map and reaching to 2245nT. This zone is connected on the surface with NSS. It may be interpreted as representing structural lows or down-faulted basement blocks. It is obvious from the regional magnetic-component map that the deep-seated magnetized masses give rise to anomalies having long wavelengths, low frequencies and weak intensities.

The careful examination of this map indicates that most of the magnetic anomalies continue to appear from the RTP magnetic map to the regional one, but with lower amplitudes and frequencies. The regional magnetic-component map shows the same number of the positive and negative (high and low) magnetic anomalous zones that were recorded on the RTP magnetic map. The shapes of some of these anomalies are-to some extent-elongated, while others are somewhat rounded. Some of the small-sized magnetic anomalies shown on the RTP magnetic map appear also on the regional magnetic map but as a single continuous and broad magnetic anomaly. This feature indicates that these small-sized anomalies have a common deep root and, therefore, could be considered of deep-seated origin.

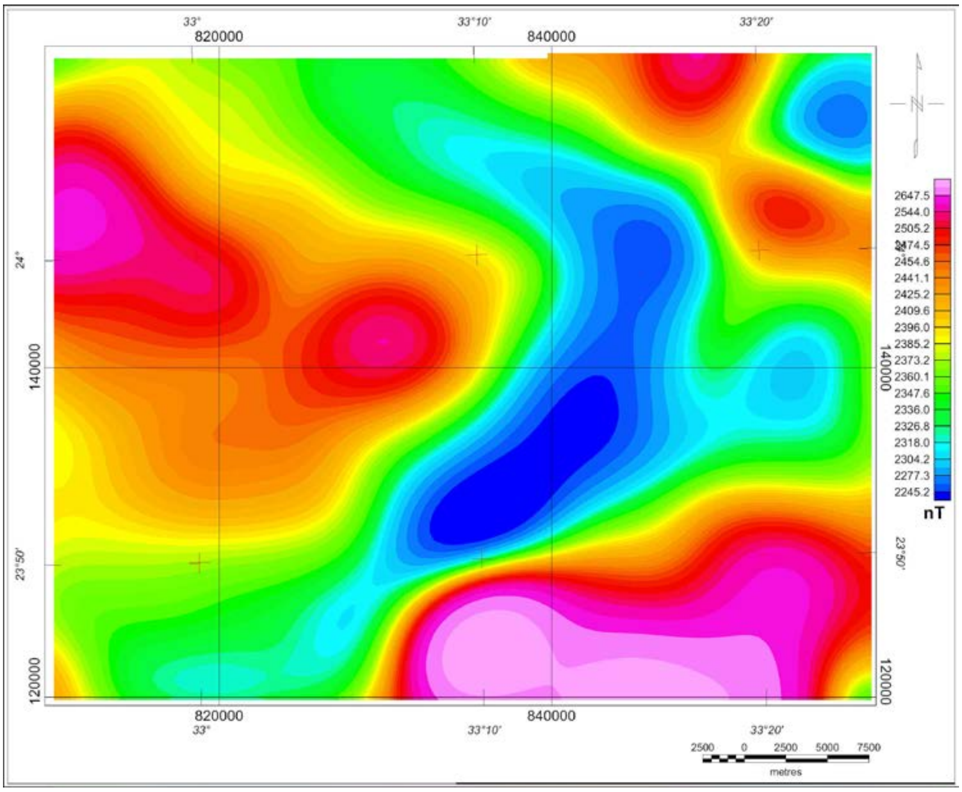

Fig. (5): Regional magnetic intensity map.

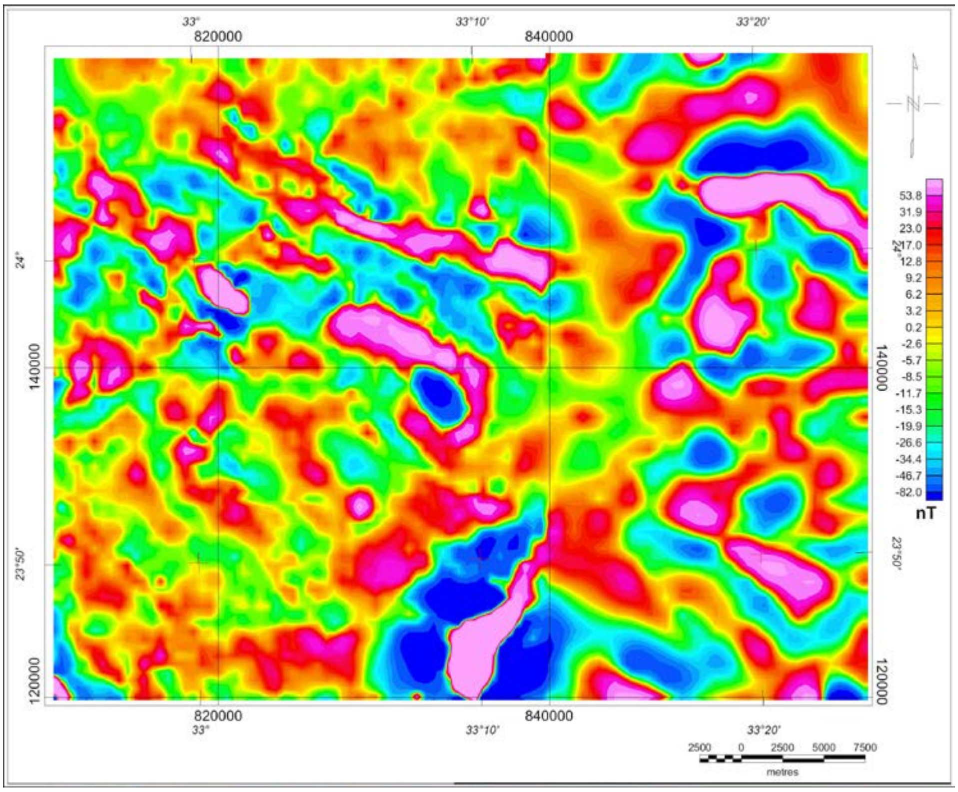

Fig. (6): Residual magnetic intensity map.

While, some other magnetic anomalies disappear on the regional magnetic-component map while they are still recorded on both the RTP and the residual magnetic-component maps. This phenomenon infers that these anomalies originate from shallow depth and are near-surface anomalies having shallow roots.

The near surface map was represented in the contour map as shown in (Fig. 6). It clearly shows several clusters of positive and negative magnetic anomalies trending NW, NE and E-W directions, which are of high resolution than the RTP aeromagnetic map. These anomalies appeared mainly as semicircular or slightly elongated in shape. The highest negative amplitude -82 nT is located in the central south and northeastern parts is closely related to the NSS as shown in the geological map (Fig.2). On the other hand, the highest positive anomalies are concentrated at the southwest with amplitude >53nT. These anomalies trend NW, NE and E-W directions and associated with the younger granites and metsediments as shown in the surface geological map.

The RTP data was continued upward at 2.0km as a filter to remove anomalies from shallow sources. It was also used to compare with the deep-seated magnetic component at the same level. Upward continuation tends to accentuate anomalies caused by deep sources at the expense of anomalies caused by shallow sources (Blakely, 1995). Comparative investigation of the reduced to pole upward continued aeromagnetic map at level 2.0km (Fig. 7) and the regional magnetic component map at the same level shows that there is a nearly great similarity between both. However, at this level of observation, the magnetic anomalies on the two maps still have approximately the same characteristics, both in areal extent, amplitude and magnetic trend. The difference in magnitude of the magnetic anomalies in some parts may be due to the difference in a logarithm of the software used for the calculation of the two processes. This map reveals the effects of deeply buried magnetized material (deep-seated) and resolved the deep major structures prevailing in the area.

The horizontal magnetic field intensity was applied to the regional magnetic component map Fig. (8). The Peaks of the HG component are trending mainly in NW, NNW, and NE directions. The method is especially useful in the case of faults (up-faulted and down faulted blocks) or discontinuities and folds (anticlines and synclines), where the isolines of horizontal magnetic gradient are closed near the plane of the fault discontinuity. The magnetic closures having the highest values were interpreted as uplifted blocks (or anticlines) while those possessing the lowest values were interpreted as subsided blocks (or synclines). The axes of these interpreted up and down-thrown blocks (or folds) are correlated well with the elongation of these magnetic closures (anomalies).

In the present work the second vertical derivative technique (SVD) of the RTP magnetic map was used to locate the edges of magnetic bodies and to emphasize sources of shallow depths. The similarity between both of the second vertical derivative and the residual map is expected; because both maps are depending on the curvature of the anomalies (Dobrin, 1976). This map shows alternative positive and negative magnetic anomalies and some high- amplitude ones, with great gradients indicating major faults. Besides, other low amplitude and gentle gradient magnetic anomalies that reflect smaller displacement faults are recorded. The careful examination of SVD map (Fig. 9) shows that the area possesses numerous major and minor positive and negative groups of magnetic anomalies with varying wavelengths and amplitudes. This variation may reflect change in the composition of rocks and their depth respectively. Consequently this map reveals the effects of deeply buried magnetized material (deep-seated) and resolved the deep major structures prevailing in the area.

The most conspicuous feature of the analytical signal map Fig. (10) is the presence of a group of positive magnetic anomalies as well as many associated negative ones, which are aligned in alternating manner. This indicated different types of intrusions having various lithologic compositions (acidic, intermediate and basic). It could be concluded that the causative bodies of most of these anomalies are dyke like bodies with no deep root i.e. either outcropping or existing at shallow depths beneath the surface. It is very noticeable that the contact between the basement and sedimentary rocks is well pronounced and visible on the analytical signal map Fig. (10). A well-defined boundary with appreciably different degrees of magnetic relief can be easily traced in this contact zone. This may reflect a contrast between the magnetic properties of rocks along the opposite sides of this boundary and indicate also the existence of a major fault. The eastern part of the study area, which is represented on the surface by NSS and Quaternary sediments is occupied by a broad belt of moderate to strong negative magnetic anomalies having nearly NW direction and characterized by their long wavelength and low magnetic relief.

The integration of the results obtained from the previously mentioned techniques help to constructing the basement tectonic map for the studied area.

6. Interpreted Basement Tectonic map

The basement tectonic map for the studied area was constructed using the information resulted from the previous analysis applied to the aeromagnetic data and integrated with surface geologic information Fig. (2). A close examination of the interpreted basement tectonic map Fig. (11) illustrates that the study area is characterized mainly by the presence of two intersecting sets of NNW-SSE to NW-SE and NNE-SSE to NE-SW trending major faults as following:

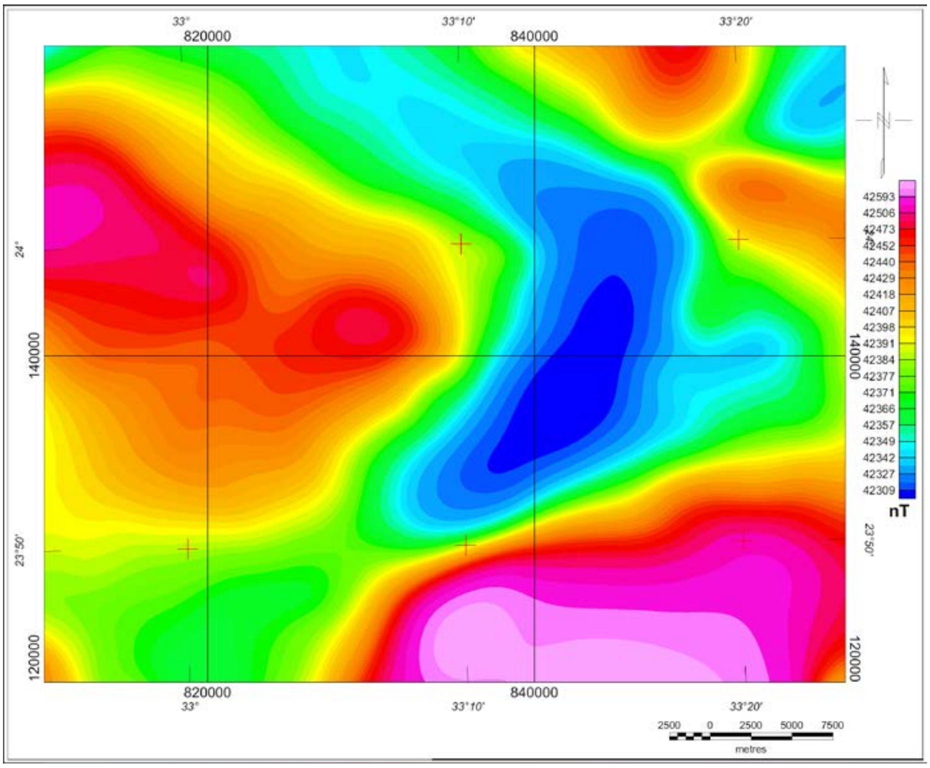

Fig. (7): Upward continuation for the magnetic intensity map at 2km.

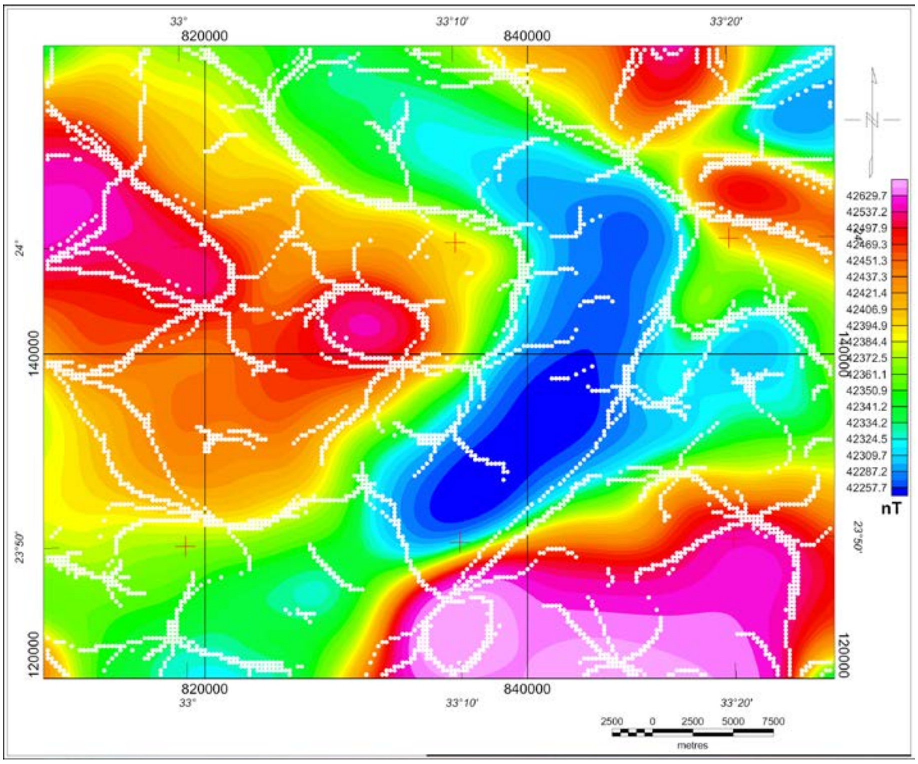

Fig. (8): The picked maxima of the horizontal gradient function over the regional magnetic component map.

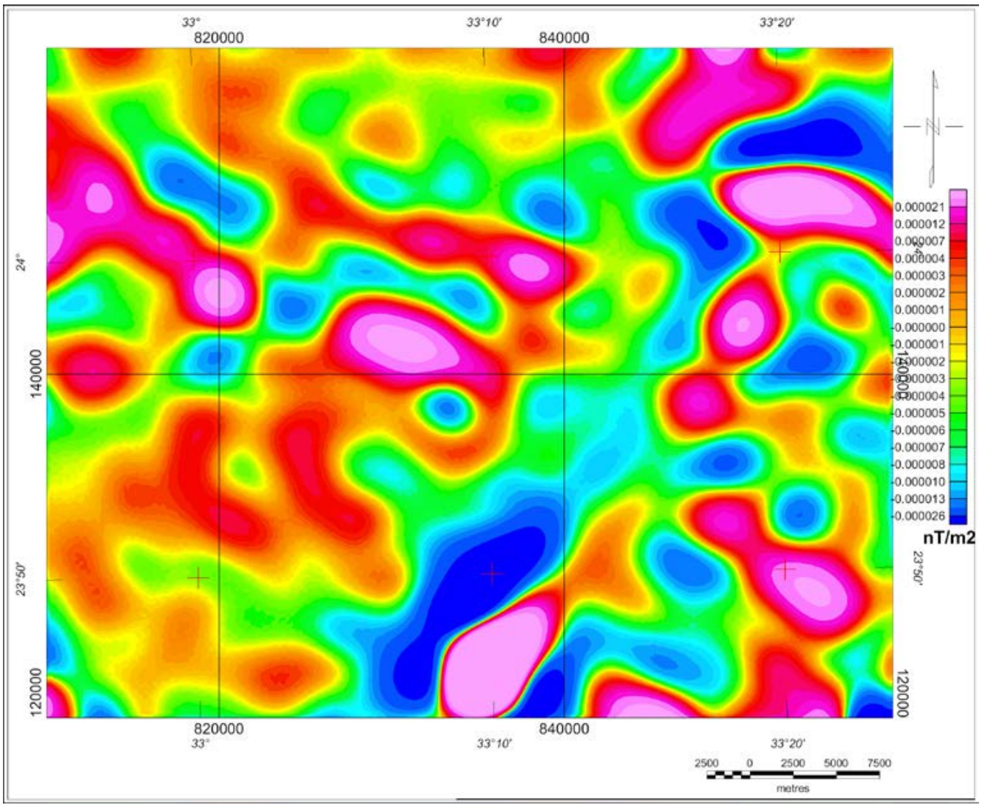

Fig. (9): The second vertical derivative (SVD) over the regional magnetic component map.

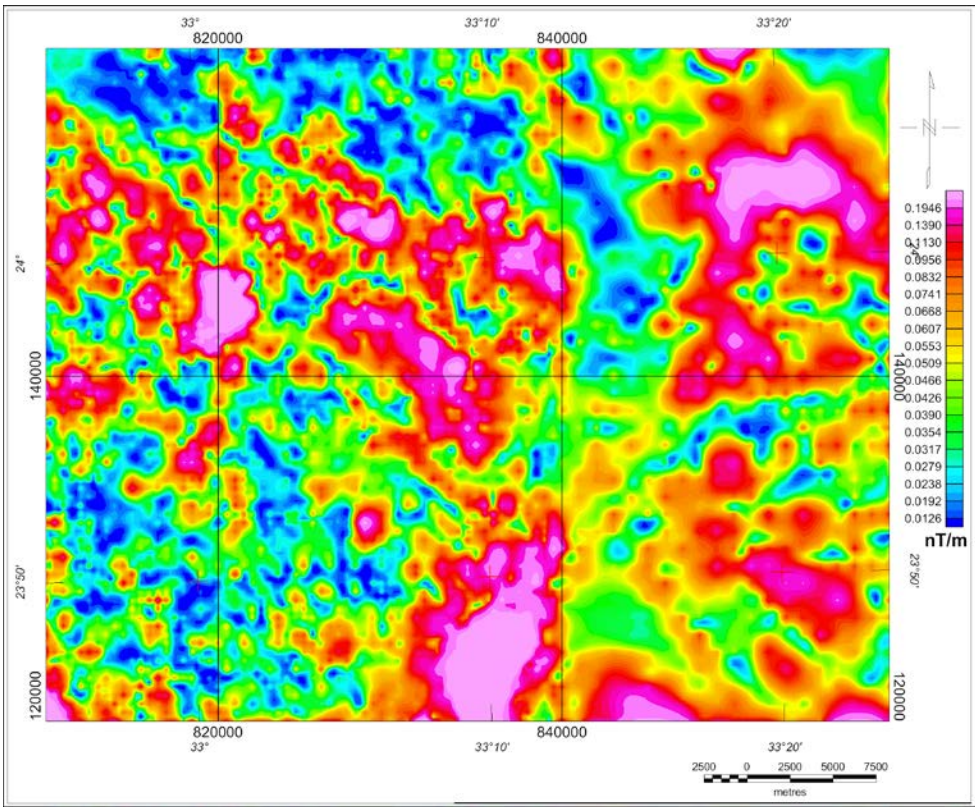

Fig. (10): The analytical signal over the RTP total magnetic intensity map.

The first interpreted group of faults with NNW-SSE to NW-SE include five strike slip faults, clearly appear at the north of the map running through the whole area, and are related to the development of the Red Sea. The second interpreted group of faults with NNE-SSE to NE-SW includes six strike slip faults at the south of the map. The trend of this group of faults is comparable with the Gulf of Aqaba trend.

The magnetic signature of the aeromagnetic maps shows several alternative high and low magnetic zones. The magnetic low zones are supposed to represent structural lows (down-faulted blocks, grabens or synclines), while the magnetic high zones, separating them represent structural highs (uplifted blocks, horsts or anticlines). The distinct boundary between zones with different magnetic characters may indicate the presence of a major basement fault and/or a contact.

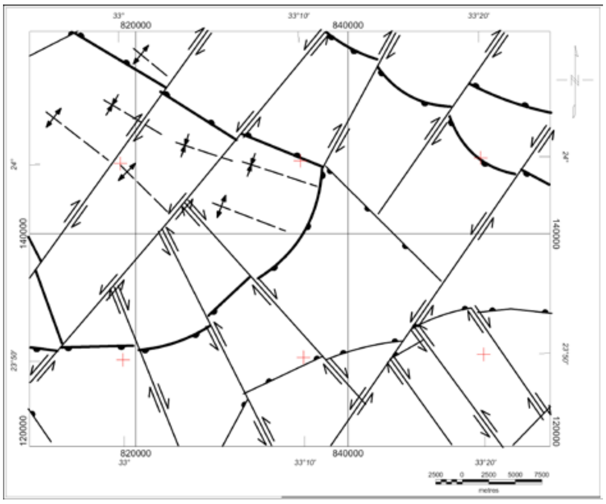

Fig. (11): The interpreted basement tectonic map of the study area.

In the present study, trend analysis technique was applied on the resultant structural elements, to define the predominant tectonic trends affecting on the area. As a result of the application of rose diagram technique (Fig. 12). Five main trends were proved to be significant, which are sorted from the strongest to the weakest as, NW, NE, WNW and NNE. Statistical trend analysis of the fault axes of the major uplifted and subsided blocks shown in the basement tectonic map revealed that there is a strong relation between magnetic and structural trends. This analysis shows two major NE and NW structural orientation. In the Eastern of Aswan area two broad groups of folds have been traced. The older group is found only in the basement rocks, while the younger group can be traced in the basement and overlying sediments. The fold axes of the older group trend NE-SW and NNW-SSE (Dahy et al., 2004). Folds are represented in the study area by a series of roughly parallel syncline (down-faulted blocks) and anticline (uplifted blocks) folds. These folds cut the first magnetic zone at the northwestern part of mapped area, trending in NNW and NW direction. Hasely, (1975) stated that the NNW trend is recognized as a possible significant trend in Egypt, because it may have been widely developed as a shear and drag fold direction during Jurassic and Cretaceous time as a result of the regional left lateral shear in the Tethyan region.

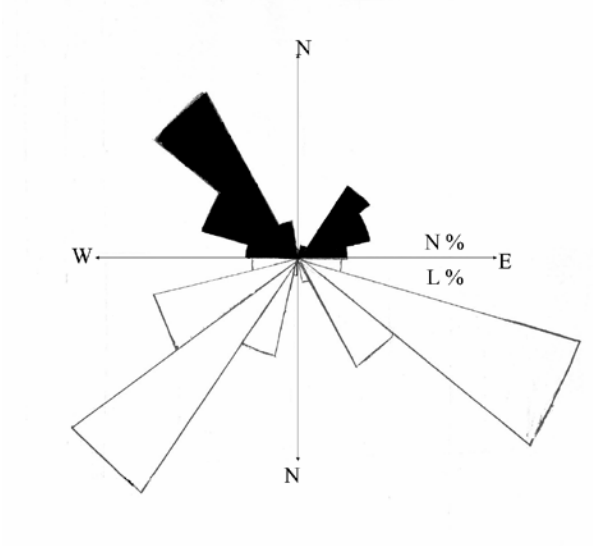

Fig. (12): Trend analysis for interpreted basement tectonic map of the study area.

The examination of the interpreted basement tectonic map can lead to see that the study area is characterized mainly by the presence of two intersecting sets of NW-SE to NNW-SSE and NE-SW to NNE-SSW trending major faults. It shows also that the main wadis in the study area (W. El Hudi, W. Sikket el Hinawya, and W. El Arab) are structurally controlled. The fault trends, which bound the main wadis in the study area, are oriented generally in NE and NW directions. El Shazly (1966) explained the NE-SW structural trends as traversal fracture to the major NW-SE fractures along which huge plutons were emplaced. The intersections between NE-SW and NW-SE deep-seated linear tectonic zones are in several cases foci of mineralization including granetic and porphyry mineralization. These large shear zones comprise large zones of highly metamorphosed crystalline basement rocks accompanied by numerous intrusions of siliceous rocks with associated metasomatism. These zones are radioactive and magnetically active, although anomalies are usually irregular (Garsori and Krs, 1976).

7. CONCLUSION

According to the visual inspections of the various geological and aerial magnetic maps, it was possible to divide the total magnetic intensity reduced to the north magnetic pole (RTP) magnetic contour map into four different magnetic zones based on the differences in the character of the magnetic patterns. Three of the identified magnetic zones are represented mainly by positive anomalies, while the fourth zone represent mainly negative ones. This map should reflect and notably register the gross structural pattern of the study area. The magnetic signatures of the aerial magnetic maps show several alternative high and low magnetic zones. The mainly magnetic–low zones are supposed to represent structural lows (down-faulted blocks, grabens, synclines or basin), while the mainly magnetic-high zones separating them are supposed to represent structural highs (uplifted blocks, horsts, domes or anticlines). These magnetic structural lineaments, which heavily dissected the RTP map are shown on the interpreted magnetic basement structural map.

The magnetic maps, revealed some structural fault zones and trends in the study area. It was possible to differentiate between some rock types according to their magnetic character. Reduced to the pole, analytical signal and second vertical derivative maps were prepared to help in visualize the gross structural framework of the area. The NW-trending faults together with the NE-trending cross faults and the oblique ones (NNE, NNW, EW and ENE) constitute the overall structural pattern of the study area. The granitic mass is affected by a coupling force which yields two major faults striking in NNW direction. The integration of the previous results obtained from the aeromagnetic survey data aided by the geological information led to the construction of the basement tectonic map. This map shows a group of fault trends. These fault lines are dissected and displaced by NW, NE, WNW and NNE fault lines.

ACKNOWLEDGEMENT

The outher is grateful to **Prof. Dr. Kadry M Fouad** Professor of applied geophysics, Nuclear Materials Authority, Cairo, Egypt for his great assistance in revision of the manuscript and encouragement at all stages in this work.

REFERENCES

Aero Service, (1984): Final operational report of airborne magnetic / radiation survey in the Eastern Desert, Egypt, for the Egyptian General Petroleum Corporation, Cairo, Egypt. Aero-Service, Houston, Texas, USA, Six Volumes.

Attia, M.I., (1955): Topography, geology and iron ore deposits of the district east of Aswan: Geol. Survey, Egypt, Cairo, 262p.

Blakely, R.J., (1995): Potential theory in gravity and magnetic applications. Cambridge University Press, Cambridge, UK.

Cianciara, B., and Marcak, H., (1976): Interpretation of gravity anomalies by means of local power spectra. Geophysical Prospecting, V.24, pp. 273-286.

Cianciara and Marcak (1979): Geophysical anomaly interpretation of potential field by means of singular points method and filtering. Geophysical Prospecting, V.27, pp. 251-260.

Cordell, Lindrith, and Grauch, V.J.S., (1982): Mapping basement magnetization zones from aeromagnetic data in the San Juan Basin, New Mexico: Society of Exploration Geophysicists, 52nd Annual Meeting, Abstracts and Bibliographies, p.246-247.

Cordell, Lindrith, and Grauch, V.J.S., (1985):Mapping basement magnetization zones from aeromagnetic data in the San Juan basin, New Mexico in Hinze, W.J., ed., The utility of regional gravity and magnetic anomaly maps: Society of Exploration Geophysicists, p.181-197.

Dahy S.A., Hassib G.H. and Haaaoup A. (2004): Identification of local observed near Aswan international airport. J. Appl. Geophys., Vol.3 No.2. pp43-50.

Dixon T.H., (1981): Age and chemical characteristics of some Pre–Pan–African rocks in the Egyptian Shield. Precambrian Research 14, 119 – 133.

Dobrin, M.B., (1976): Interpretation to geophysical prospecting. Mc Graw- Hill Book Co., New York, 445p.

Elkins T.A., (1951): The second derivative method of gravity interpretation. Engel, A.E.J.,Dixon, T.H., and Stern, R.J.,1980. Late Precambrian evolution of Afro–Arabian crust from ocean arc to craton. Geol. Soc. Am. Bull, 91 (I), 699–706.

El-Gaby, S., List, F.K. and Tehrani, R. (1988): Geology, evaluation and metallogensis of the Pan-African Belt of Notheast Africa and adjacent areas, S. El Gaby and R. 0. Greiling (Eds.), Frieder. Vieweg, Braunschwieg, Fedral Republic of Germany, 17-68.

El Ramly M.F., and M.K. Akaad, (1960): The Basement complex in the crustal Eastern desert of Egypt Between Lat. 25^{o} 30$^{/}$ and 25^{o} N. Geol. Surv. Egypt. Paper 8, 35p.

El-Shazly, E. M., (1964): On the classification of the Precambrian and other rocks of magnetic affiliation in Egypt, U.A.R, section .10, International geological congress, India, 17p;On the classification of the Precambrian and other rocks of magnetic affiliation in Egypt, U.A.R, section .10, International geological congress, India, 17p;

El-Shazly, E. M., (1977): The geology of the Egyptian region. In the ocean Basins and margins, A.E.M. Nairn, W.H. Kanes, and F.G. Stehli (Eds.), Plenum Publishing Corporation, pp. 379-444.

Halsey, G. H., (1975): Interpretation of Erts linears. Lecture delivered for Egyptian Geologists in Cairo, Egypt.

Henderson R.G., and Zietz I., (1949): The computation of second vertical derivatives of geomagnetic fields. Geophysics, 13, 508-516.

Farag, I.A.M., (1958): Stratigraphy of Egypt, Faculty of Science, Cairo Univ. Vol. 1 and Vol. 2.

Naidu, P.S., (1969): Estimation of spectrum and cross spectrum of aeromagnetic field using Fast Digital Fourier Transform (FDFT) techniques. Geophysics. Prospecting, Vol. XVII, pp. 344-361.

Reid A.B., Allsop J.M., Granser H., Millett A.J., Somerton I.W., (1990): Magnetic interpretation in three dimensions using Euler deconvolution: Geophysics, Vol. 55, 80-91.

MacLeod, I. N., joues, K., Dai, T. F.,(1993): 3D analytic signal in the interpretation of total magnetic field data at low magnetic latitudes. Exploration Geophysics 24, 679-688.

Meshref, W. M. (1990): Tectonic tramework, The geology of Egypt (Chapter VII), Ed.Rushdi Said, by A. A. Balkema/Rotterdam/ Book field, pp. 113-155/ 1990.

Garson, M.S. and Krs, M. (1976): Geophysical and geological evidence of the relationship of Red Sea traverse tectonics to ancient fracture, Geol. Soci. Am. Bull. vol. 87 pp. 169-181.

Gunn O.J., (1975): Linear transformations of gravity and magnetic fields. Geophysics. Prosp. 23, 300–12**.**

Issawi, B. (1978): Geology of Nubia west area, western desert, Annals of the Geological Survey of Egypt.

Issawi, B. (1982): Geology of the southwestern desert of Egypt, Ann. Geol. Surv. Egypt.

R. Said, (1962): The Geology of Egypt, Elsevier, Amsterdam, 1962, 377 pp.

Shuang Qin, (1994): Analytical signal approach to interpretation of the total field magnetic anomalies:Geophy. Prospecting V.42 pp.665-675.

Takla, M. A. and Hussein, A. A.(1995): Shield rocks and related mineralization in Egypt. 11th sympo. Precamb. Develop., Cairo, Egypt, Abst.,pp.6-7.

Vacquier V., Steenland N.C., Henderson R.G, and Zietz I., (1963): Interpretation of aeromagnetic maps. Geol. Soc. of America. Memoir 47.